A Spatiotemporal Analysis of Changes in Forest Extent of the Northern Front Range, CO

Researchers and Affiliations:

Kyle C. Rodman* – Department of Geography, University of Colorado at Boulder.

Thomas T. Veblen – Department of Geography, University of Colorado at Boulder.

*PI Contact Information - Phone: (719) 648-9957. Email: Kyle.Rodman@colorado.edu. Current Address: Department of Geography, University of Colorado at Boulder, 260 UCB, Guggenheim 110, Boulder, CO. 80309-5002, USA.

Abstract:

Forests are dynamic ecosystems that experience constant fluctuations in structure, composition, and extent. Though much is known about disturbance regimes and landscape change in the northern Front Range of Colorado (NFR), there currently is no quantification of the extent of forest cover change for the NFR from the early 1900s to the present. Herein, we combine repeated landscape photography and aerial photography to assess changes in forest extent across the NFR over the past century. The data included in these analyses are spatially comprehensive, covering 320,000 ha, and in the future may be paired with data from 66 field sites in which stand ages and fire scars were extensively sampled, or with models derived from these data. Oblique landscape photos provide a unique and important contribution to this work by extending the temporal coverage of the data (ca. 1900 to present), and providing useful records that can be utilized by local managers for interpretation and outreach. Preliminary results suggest slight increases in forest cover across OSMP properties surrounding Boulder, CO, and a majority of these properties (>87%) meet previously established criteria suggesting that fuel treatments and forest restoration are convergent goals.

Introduction

Forests are constantly changing in response to climatic factors, ecological disturbances, and patterns of human land use (Hansen et al. 2013). These dynamic ecosystems are crucially important to the earth's biosphere, providing habitat for countless wildlife species (FAO 2015), playing a major role in the global carbon cycle (Bonan 2008), protecting watershed quality (Rocca et al. 2014), and supplying numerous economic, social, and spiritual benefits. Because of this, ecologists have long been interested in forest dynamics (Attiwill 1994). While past ecosystem behavior is not a perfect analog for the future (Millar et al. 2007), retrospective studies using tree ring data, charcoal, pollen, and historical documents and photos can still provide important insight into the way that forest ecosystems may respond to future events, improving modeling efforts, and better defining lines of future inquiry (Swetnam et al. 1999, Hayward et al. 2012). While much is known about the historical ecology of conifer forests in the northern Colorado Front Range (NFR; Veblen and Donnegan 2005, Kaufmann et al. 2006), the basis for our knowledge is primarily derived from localized case-studies or samples from the broader landscape. In this project, we have the goal of developing seamless maps of forest cover across the NFR for the time-periods of 1938, 1999, and 2015, which will be useful for comparison with patterns of the potential drivers of forest change (climate, disturbance, and development). We have also paired these images with oblique landscape photos, captured ca. 1900 and 2016.

Wildfire and Disturbance in the NFR

Wildfire is one of the most important terrestrial disturbances (Bowman et al. 2009), and has played a key role in forests of the NFR (Veblen and Donnegan 2005). Prior to the 20th century, fires were relatively frequent and of low-moderate severity in low elevation montane forest and grassland sites (below 2260 m), but fire severity typically increased with elevation, and high-elevation coniferous forests often experienced large, high severity fires initiated by extreme drought (Sibold et al. 2006, Sherriff et al. 2014). The mid-late 1800s were a time period of heightened fire activity in the NFR concurrent with widespread droughts throughout the Rockies (Veblen et al. 2000, Kitzberger et al. 2007, Sherriff and Veblen 2008, Schoennagel et al. 2011, Gartner et al. 2012). These decades were also coincident with increases in logging, mining, and other impacts from Euro-Americans, which demonstrated visible influences on forest structure (Veblen and Lorenz 1986, Veblen and Donnegan 2005). This period of enhanced fire activity (*Era 1*: ca. 1850 – 1920) was followed by the fire exclusion era (*Era 2*: 1920 – 2000), in which relatively few fires burned across much of the NFR, likely due to a combination of direct fire suppression, grazing by cattle and sheep, lack of combustible fuels in higher, recently burned sites, and unsuitable climatic conditions for ignition and spread. The relative ecological impact of this gap in fire activity varies from low to high elevation sites, and forests at the lower extent of ponderosa pine (*Pinus ponderosa*) are considered to have deviated most substantially from their natural ranges of variability (Platt and Schoennagel 2009, Sherriff et al. 2014). So, while forest cover across the NFR has undergone considerable change over the past century, the relative influence of Euro-American fire exclusion varies at a coarse-scale along the elevation-climatic gradient and at a fine-scale due to local topographic variability.

Since ca. 2000, there is mounting evidence that we have entered a third era in the forests of the American West and in those of the NFR, one in which anthropogenic climate change may be the most important driver of ecosystem change. Across much of the western United States, the area burned in large wildfires has increased since 1984 (Dennison et al. 2014), and more than 50 percent of the area burned in this time period can likely be attributed to anthropogenic climate change, rather than just natural climate variability (Abatzoglou and Williams 2016). Similarly, bark beetle outbreaks (*Dendroctonus* spp. and *Ips* spp.) can transition from endemic to epidemic levels with warmer temperatures and increased drought stress (Breshears et al. 2005, Raffa et al. 2008), and the area attacked by beetles has expanded in recent years (Bentz et al. 2010, Chapman et al. 2012). Because many disturbance types (e.g. fire and insect outbreaks) are predicted to increase under continued climate warming, it is important to understand the effect these events have on forest structure and subsequent successional trajectories (Turner 2010).

Past Forest Change in the NFR

Previous studies of the changes in forest cover and structure across the NFR have used historical documentary sources, historical aerial and oblique landscape photography, dendrochronological data, and remote sensing techniques, but have been spatially and/or temporally limited. Veblen and Lorenz (1986, 1991) paired historical landscape photos (ca. 1900) with contemporary photos (ca. 1980), tree ring data, and historical records of land use to describe structural changes in montane and subalpine forests of the NFR. A series of studies published by members of the Veblen Lab at CU between 2000 and 2012 have used tree-ring methods to document spatio-temporal patterns of fire history and associated changes in forest structure across Boulder County in the lower and upper montane zones (Veblen et al. 2000, Sherriff and Veblen 2006, 2007, Schoennagel et al. 2011, Gartner et al. 2012). Recent tree-ring based research performed by a different research group suggests similar trends in lower montane zone of Boulder County (Brown et al. 2015). The extensive tree-ring dataset of the CU group has recently been used for a comprehensive spatial reconstruction of historical fire severity and its comparison with actual and potential modern fire severity across the montane zone of the NFR (Sherriff et al. 2014). With a slightly different approach, Williams and Baker (2012) used

General Land Office records and associated bearing tree information to quantify historical forest structure and fire regime class in the NFR. Despite the differences in data sources and analytical methods, these aforementioned studies are cohesive in that they demonstrate two important findings: 1) Conversion of some grassland sites to forests at lower elevations. 2) Increasing fire severity and decreasing frequency with elevation, with montane forests in the NFR showing a wide range of historical fire regimes.

The air photo approach has been successfully utilized in previous work in the NFR, and provides substantial increases in spatial resolution and extent when compared to other data sources. Mast et al. (1997) used manual photo interpretation, historic maps, and a binary remote sensing classification of forest vs. non-forest to quantify tree invasion into grasslands at three study areas in lower montane forests surrounding Boulder, CO, 1937-1991. Platt and Schoennagel (2009) expanded upon this approach by developing a sophisticated classification algorithm, and surveying 39 separate sites across the montane zone in Gilpin, Jefferson, Boulder, and Larimer counties. Our approach combines image classification of 308 of these air photos with oblique landscape photography and extensive field data, providing seamless estimates of land cover across broad spatial (ca. 320,000 ha) and temporal (1938-2015) extents. Specifically, we had the following objectives: *1) Assess changes in forest extent across the NFR using oblique landscape photos and aerial photos. 2) Determine the spatial associations of historical fire regime, recruitment pulses, and topographic position with changes in forest extent across the study area (1938-1999). 3) For the most recent time period of analysis (1999-2015), assess the effects of wildfires and bark beetle outbreaks on changes in forest extent.*

Methods – Landscape Photos

Data Acquisition – In databases managed by the Boulder Public Library, the Denver Public Library, and the Colorado Historical Society, we performed a targeted search for landscape photos covering portions of Boulder OSMP properties. Many of the images contained in these databases were captured by early photographers in the Boulder area - such as William Henry Jackson and Joseph Sturtevant - between 1890 and 1910. Veblen and Lorenz (1986, 1991) previously collected ~70 of these repeat landscape photos, and our recent collection provides 20 additional image pairs in the areas surrounding Chautauqua, Flagstaff Mountain, Settler's Park, and Mount Sanitas in Boulder County, CO.

Photo Re-location and Image Processing – Following the identification of images in library databases, we acquired low-resolution digital scans of these images and re-located the approximate location of the original photo. When the original photo location was obstructed by vegetation or recent development, we located the nearest suitable site and repeated the image from a slightly different vantage point. During photo collection, we also recorded UTM coordinates and elevation for each photo point for future use. We collected imagery in the field during the time of day that best re-created the original exposure, typically early to mid-morning. After image collection, we manually aligned and cropped the recently collected image to match the historical photo. When historical and contemporary images provided a reasonable match and were judged to be useful, we requested or purchased high-resolution copies of these images from library collections to facilitate reproduction and printing.

Methods – Air Photos

Study Area – Our study area for the aerial photos encompasses ~320,000 ha in Boulder, Clear Creek, Gilpin, Jefferson, and Larimer Counties, and ranges 39.7-40.7° N, and 105.2-105.6° W (Figure 1, Table 1). Climate varies widely across the region, and elevations in the study area range 1600-4200m. Along this elevational gradient, vegetation in the study area begins with short grass prairie at the lowest sites, transitioning into lower montane forests (principally dominated by *Pinus ponderosa*) and upper montane forests (*Psuedotsuga menziesii* and *Pinus contorta*, with fewer *Pinus ponderosa*). At the highest forested sites, *Pinus flexilis*, *Abies lasiocarpa*, *Pinus contorta*, and *Picea engelmanii* are commonly found, giving way to alpine vegetation at ca. 3400m (Kaufmann et al. 2006). Euro-American settlement of the NFR rapidly increased in the mid-1800s, and logging and mining impacts are widespread, with recovery rates from these anthropogenic disturbances varying across the landscape (Veblen and Lorenz 1986).

Datasets – We acquired aerial images and GIS datasets for the study area from several sources. Historical air photos were available through the University of Colorado Boulder Library, and were originally captured in flights by the United States Department of Agriculture in 1938 and 1940 (Figure 1; Table 1). Though the images were acquired in separate time periods, only one flight line of 35 photos was collected in 1940 (the majority having been captured in 1938). The UC Boulder Library scanned and digitized over 1,700 individual images from this time-period, covering much of the NFR. The scanned images are between 1.2 and 1.4m in nominal ground resolution, with pixel size varying based on camera altitude and ground surface elevation. The aerial photo program was originally established to inventory timber stands and monitor agricultural areas (Matthews 2005), and has continued to operate intermittently within the NAPP and NAIP (National Aerial Photography Program and National Agricultural Imagery Program, respectively). Therefore, we acquired data from the NAPP (1999, greyscale), and NAIP (2015, 4-bands in visible and near infrared portions of the spectrum) to compare with historical imagery. These recently collected datasets have 1m spatial resolution.

For later use in GIS analysis, we have obtained several ancillary datasets. These include digital elevation models (10m) from the US Geological Survey (USGS 1999), as well as current land cover and vegetation data from the National Land Cover Dataset (Homer et al. 2015), and LANDFIRE (Rollins 2009). We also obtained layers describing the locations of water bodies and building footprint and parcel data from county and city GIS databases, road data from Open Street Map, and LiDAR-derived canopy height models that cover city open space properties in the foothills near Boulder, CO. Additionally, we have identified 66 separate field sites in which data were collected to summarize fire history and stand ages (Figure 1). These sites were a subset of those synthesized in Sherriff et al. (2014), and were selected because they were within the footprint of the available aerial photos. These sites, as well as the model of fire regime class created from them, have yet to be directly compared to changes in land cover and forest extent.

Air Photos, Data Processing and Analysis – Following data acquisition, we georeferenced the historical air photos using metadata from each image that described the approximate center location of the frame. The images were originally provided in .jp2 format, and we converted them to the geotiff format while projecting the data to the NAD83, UTM zone 13N. We later mosaicked individual flight lines of images collected on the same dates (11 total image "strips") using a spline transformation with nearest neighbor re-sampling and at least 40 tie points in overlapping areas shared between adjacent images. The next step in this process is to stitch and mosaic individual flight lines to one another. We will perform this mosaicking in a similar manner to that described above, and will then use Adobe Photoshop CS6 to correct for tonal differences and inconsistencies in the final image. The DOQ (1999) and NAIP (2015) imagery is already georeferenced, orthorectified, and available in the UTM projection. The dependent variable in these analyses is percent forest cover (canopy cover) in an aggregated pixel, where spatial resolution of the dataset will be based on the accuracy of georeferencing between historical and contemporary imagery (likely in 100m x 100m cells).

Following Coburn and Roberts (2004), we used an expanding-window method to describe the variance in tonality (pixel brightness values) around each pixel in each image. In short, this method computes the mean and standard deviation of pixel brightness values in 3x3, 5x5, 7x7, 9x9, 11x11, 13x13, and 15x15 pixel windows surrounding each cell in the original data, then summing the result of all operations. We computed the local standard deviation to aid in differentiating between cover types that have similar spectral characteristics but different levels of local variation. This approach was experimental but demonstrated promising results for some of the available imagery, and appears particularly useful when differentiating between dark, homogeneous areas (such as shadow or water), and dark areas with variance (forests).

Similar to Platt and Schoennagel (2009), we also identified dark pixels surrounded by light areas in an effort to improve the classification of individual trees that may appear spectrally different than patches of dense, contiguous forest. This method also uses an expanding window approach, and utilizes the mean and standard deviation from each window as follows: $if\big(x < (\mu - 2\sigma)\big)\{cv = cv + 1\}\ else\ \{cv = cv + 0\}$, where x is the value of cell being considered, cv is the cell value in the "darkness" layer, μ represents the mean within the window of a given size (3, 5, 7, 9, 11, 13, 15), and σ is the standard deviation of pixel values in this same window. So a pixel is considered to be significantly darker than its surroundings it if it has a value lower than the the window mean (μ) minus two standard deviations (σ). These calculations are then summed across all window sizes. We completed these analyses in Python 2.7, using the GDAL (Geospatial Data Abstraction Library), SciPy, and NumPy modules. We have also experimented with image segmentation methods that group pixels with relatively similar values together into objects (e.g. segment mean shift, k-means). This approach has gained popularity among analysts working with high-resolution data, and may be especially useful due to tonal differences between similar cover types on different slopes and aspects and image tiles. Segmentation may also account for poor image quality in portions of the historical air photos (Platt and Schoennagel 2009). It is also possible to incorporate the size and shape (circularity, rectangularity) of segmented objects into the final classification.

To test the more traditional pixel-based approach to image classification (rather than an object-based one), we selected training pixels along a East-West transect of imagery tiles in Boulder County. We selected the location of these transects with the goal of obtaining a representative sample of the larger geographic region of the NFR. The transects include areas of sparse forest cover at lower elevations as well as dense, relatively homogeneous forests at higher elevations. These sample areas are also topographically complex, having wide variations in slope angle and aspect which leads to differences in lighting conditions. Because the goal of this project is to distinguish forest cover from the surrounding areas without forest cover, we visually identified three distinct cover types. These cover types were forest, non-forest (roads, bare ground, and grassland) and water/shadow. Along this transect, we selected 100 pixels each of the three different cover types from each set of imagery (1938, 1999, 2015).

Next, we developed a decision tree classification for each set of imagery (1938, 1999, 2015) based on a conditional inference framework. Similar to random forests, conditional inference is an iterative machine learning procedure that identifies important variables, as well as the interactions between variables in complex, multivariate datasets (Breiman 2001, Hothorn et al. 2014). Conditional inference and random forests are useful for the purpose of remote sensing classification because they identify optimal binary splits of values that best differentiate between known classes (Horning 2010), in this case forest, non-forest, and water/shadow. Ancillary data such as slope, elevation, aspect, climate, or landcover classification can also be incorporated to improve upon the spectral classification, though we did have not yet completed this for this analysis. We used conditional inference trees in the "party" package (Hothorn et al. 2014) and assessed model fit using the "caret" package (Kuhn 2015), both in the R environment. Following development of the classification scheme, we performed a classification in a separate geographic region. In this region, an additional East-West transect in Boulder County, we visually identified 300 pixels each of the three cover types (900 total) for model validation and accuracy assessment. We then calculated producer's and user's accuracy for the classification using these pixels within confusion matrices for each set of imagery (1938, 1999, 2015). As further validation of the 2015 NAIP classification, we compared our results to the area of OSMP properties occupied by tree crowns identified through the previous canopy segmentation of LiDAR products.

To present preliminary results of the analysis, we compared classification results for the 1938 and 2015 imagery covering OSMP properties. OSMP properties were initially included in this analysis if they were within the extent of the 1938 imagery, and had visible conifer forest cover during one of the time periods. We then removed small, isolated parcels, and merged small parcels (< 10 ha) that share a boundary with an adjacent property to compensate for slight misalignment between image sets. Next, we performed the pixel-based classification using decision rules developed in the conditional inference analysis described above. The decision thresholds differed between image sets (1938, 1999, 2015). We also developed a mask layer combining shadows, water bodies, and building footprints within OSMP properties. Because these features can be misclassified as forest, we excluded them from later analysis of all image sets. For unmasked portions of Boulder OSMP properties, we then calculated the proportion of forest cover as the number of forest pixels out of the total number of pixels within a parcel.

Results

Repeat Landscape Photos: Completed – We located and repeated over two dozen historical landscape photos from Boulder OSMP properties (Figure 2, Table 2). Of these, we have selected the 20 historical images most suitable for future use by park staff and open space offices, and have acquired high-resolution copies of these images from library collections. At each photo point we collected multiple images, thus the final presentation of our results includes 31 image pairs (from 20 unique historical photos). We will provide lower-resolution (Appendix A) and higher-resolution copies of historical and contemporary photos, and point locations and metadata for each repeat photo point to OSMP staff. The licenses for use of these images are held by the Boulder Public Library and Denver Public Library, but are open for non-commercial use and outreach purposes.

Our results are largely compatible with previous findings (Veblen and Lorenz 1986, 1991), showing 20th century encroachment of native conifers in some low-elevation sites and those adjacent to grasslands, as well as an increase in forest cover within the city limits of Boulder due to planting of non-native deciduous species. Broad-scale development and urbanization is visible in many of the images, but some areas have changed little since 1900, providing an interesting contrast. Quantitative methods have been developed to compare repeat oblique-angle photography to analyze landscape change (Rhemtulla et al. 2002), and in the future, we will assess the potential of these methods for use with these image pairs.

Classify Aerial Photos and Compare to Recent Change: In Progress – Following acquisition of imagery (Figure 3), we developed two classification methods (one implemented, one proposed) to analyze changes in forest extent in the NFR. Our pixel-based estimates of forest cover suggest moderate increases in forest cover from 1938 – 2015. Total forest cover on the OSMP properties included in the analysis increased from 31.07 to 40.33 percent (Table 3), but variability is evident across much of the study area (Figures 4-5). The most notable areas of increase were the forest-grassland ecotone in South Boulder, the slopes of Mt. Sanitas, and the foothills south of Boulder Canyon. Results varied across OSMP properties, with some parcels showing substantial increases, and others showing substantial declines. Upon visual inspection, the property showing the greatest declines in forest cover (ERNI) had a darker tone than much of the 1938 imagery, and forest was overclassified in this area in 1938. Thus, forest declines in this area are likely overestimated.

The pixel-based classification method has shown promise, with user's accuracy for the forest class at 80%. However, producer's accuracy is lower (58%), primarily due to many shadows and water bodies being falsely identified as forest. However, these features represent a low proportion of the landscape, and the incorporation of DEMs and GIS layers with information on water bodies is likely to reduce these effects. The kappa statistic for the 1938 imagery was 0.795, suggesting substantial agreement between the observed and expected classes of validation pixels. Users accuracies for forests in the 2015 imagery are higher (95%), and local variance appeared to be more helpful in developing these classifications than in the 1938 imagery (not shown). Kappa values for the 2015 imagery were even higher than the 1938 dataset at 0.835. Grasslands and bare ground could be effectively distinguished in all imagery sets (>=85% user's and producer's accuracies in all image sets). The 2015 NAIP classification was closely aligned with the results of LiDAR canopy segmentation, where LiDAR predicted 41.92 percent forest cover across the OSMP properties analyzed and NAIP classification predicted 40.33 percent canopy cover. While accuracies for this classification are high, there are notable errors in classification on highly illuminated and dark hill slopes. The forest cover type tended towards overclassification on north-facing slopes and underclassification on south-facing slopes.

These results are presented with a couple caveats. First, we assessed classification accuracy with a subjectively selected set of validation pixels that are clear examples of each class (forest, non-forest, and shadow/water). Future accuracy assessments will require a greater number of validation pixels in each class, and randomly selected sets of pixels following classification. Thus, our estimated accuracies may be higher than those demonstrated in the actual classification. Secondly, we have not yet incorporated local minima to identify individual trees surrounded by grass or lighter-colored land surfaces, and this is likely to improve the classification in areas with sparse forest cover. Our proposed classification that incorporates DEMs and image segmentation is likely to account for tonal differences between image frames, yielding a more consistent classification across the study area, and accounting for illumination differences on north and south-facing aspects and between image frames (Figure 6, Figure 7). The end result of this classification will yield high-resolution estimates of changes in percent forest cover that can be incorporated into a land-management framework. The dataset will also be useful to other researchers studying urbanization and changes in land cover across the region.

Conclusions

Forests in the NFR have experienced substantial change over the last two centuries due to changes in climate, patterns of disturbance, and human land use. Locally, OSMP properties have experienced slight increases in forest cover between 1938 and 2015. Sherriff et al. (2014) suggest that areas under 2260m are those in which restoration and fuels mitigation are most likely to be convergent goals, and 87.64% of the OSMP properties analyzed meet this criteria. In short, thinning and burning may simultaneously accomplish the objectives of forest restoration and fuels reduction on the majority of OSMP properties. However, the increases in forest cover are generally modest (<10%), and fuel treatments must be weighed with several other management objectives - notably recreation, wildlife, climate resilience – as well as financial considerations. In addition, certain areas have experienced more dramatic change, and may be a higher priority than other sites within the jurisdiction of OSMP.

The proposed classification methods described herein demonstrate promise with all sets of imagery (1938, 1999, 2015), but steps remain before this analysis can provide final results across the study area. Upon completion, this dataset will prove useful to scientists and managers in the NFR when developing plans for forest restoration and fire mitigation treatments, and in developing an improved understanding of the drivers of landscape change. Repeat landscape photos provide a supplement to previous work in the NFR, and we will provide digital copies of 20 sets of repeat landscape photos to Boulder OSMP for use in interpretation. The licenses for use of these images are held by the Boulder Public Library, and Denver Public Library, but are open to non-commercial use and outreach.

Status of Work, and Next Steps

Deliverable	Status	Description	Delivery
Final Report and Photos to OSMP	Partially Complete	We have provided historical and contemporary repeat photographs to OSMP officials. Prints of these images can be made upon request. The aerial photography component is partially complete.	Summer 2017
Presentation at Annual Research Symposium	On Track	Oral presentation of research findings at the annual research symposium. Provides outreach to the community and to local managers.	Feb./Mar. 2017
Peer-reviewed Manuscript	On Track	From this project, we will produce at least one manuscript for publication in a peer-reviewed journal	Dec. 2017

The aerial photography component to this project is partially complete, and the goals laid out within this report can be realistically accomplished by Summer 2017. The steps to completion are as follows:

1) Complete image processing and mosaicking – Each frame in a given flight path has been combined into a larger mosaic (n = 11), and these mosaics must now be aligned with one another and tonally corrected prior to final classification of the study area (Figure 1, Figure 5). This process is ongoing, and we recently received a small amount of funding from the University of Colorado Boulder to provide salary for undergraduate assistance on the project during this academic year.
2) Perform image classification – We have calculated local variance and local minima within each image (n = 308) prior to mosaicking, thus this portion of pre-processing for the project is complete. Following creation of the 1938 mosaic, we will perform image segmentation to identify contiguous areas with similar values in brightness, variance, and context (local minima; Figure 6). We will also perform these operations on 1999 and 2015 imagery at the same spatial resolution as the final 1938 mosaic (likely 1.5 m). These imagery sets (1999 and 2015) have already been acquired and combined into mosaics covering the study area extent. Following classification, we will then perform change detection analyses at an aggregated scale, where pixel-size of the model will be based on the estimated alignment between 1938, 1999, and 2015 imagery. We will then pair our findings with stand-level data on fire history and tree establishment, or with a model derived from these data, to assess the influence of historical fire regime on 20th-century forest change. Lastly, we will use publically available GIS data from 2000-2015 to assess the drivers of forest change during this time-period.

3) Assess the potential for quantitative analysis using the repeat landscape photos – Rhemtulla et al. (2002) outline a method for using landscape photos to quantitatively assess land cover change, however their data were located at the exact point of original image capture, and closely mimicked the original image collection. Therefore, a quantitative analysis of our imagery may not be feasible, still, we will assess the utility of this approach, likely through an independent undergraduate research project.

Citations

Abatzoglou, J. T., and A. P. Williams. 2016. The Impact of Anthropogenic Climate Change on Wildfire Across Western US Forests. Proceedings of the National Academy of Sciences In press.

Attiwill, P. M. 1994. The Disturbance of Forest Ecosystems: The Ecological Basis for Conservative Management. Forest Ecology and Management 63:247–300.

Bentz, B. J., J. Régnière, C. J. Fettig, E. M. Hansen, J. L. Hayes, J. A. Hicke, R. G. Kelsey, J. F. Negrón, and S. J. Seybold. 2010. Climate Change and Bark Beetles of the Western United States and Canada : Direct and Indirect Effects. BioScience 60:602–613.

Bonan, G. B. 2008. Forests and climate change: forcings, feedbacks, and the climate benefits of forests. Science 320:1444–1449.

Bowman, D. M. J. S., J. K. Balch, P. Artaxo, W. J. Bond, J. M. Carlson, M. A. Cochrane, C. M. D'Antonio, R. S. DeFries, J. C. Doyle, S. P. Harrison, and others. 2009. Fire in the Earth system. Science 324:481–484.

Breiman, L. 2001. Random Forests. Machine Learning 45:5–32.

Breshears, D. D., N. S. Cobb, P. M. Rich, K. P. Price, C. D. Allen, R. G. Balice, W. H. Romme, J. H. Kastens, M. L. Floyd, J. Belnap, J. J. Anderson, O. B. Myers, and C. W. Meyer. 2005. Regional vegetation die-off in response to global-change-type drought. Proceedings of the National Academy of Sciences of the United States of America 102:15144–15148.

Brown, P. M., M. A. Battaglia, P. J. Fornwalt, B. Gannon, L. S. Huckaby, C. Julian, and A. S. Cheng. 2015. Historical (1860) Forest Structure in Ponderosa Pine Forests of the Northern Front Range, Colorado. Canadian Journal of Forest Research 1132:1121–1132.

Chapman, T. B., T. T. Veblen, and T. Schoennagel. 2012. Spatiotemporal Patterns of Mountain Pine Beetle Activity in the Southern Rocky Mountains. Ecology 93:2175–2185.

Coburn, C. A., and A. C. B. Roberts. 2004. A multiscale texture analysis procedure for improved forest stand classification. International Journal of Remote Sensing 25:4287–4308.

Dennison, P. E., S. C. Brewer, J. D. Arnold, and M. A. Moritz. 2014. Large wildfire trends in the western United States, 1984-2011. Geophysical Research Letters 41:2928–2933.

Food and Agriculture Organization of the United Nations. 2015. . http://www.fao.org/forestry/en/.

Gartner, M. H., T. T. Veblen, R. L. Sherriff, and T. L. Schoennagel. 2012. Proximity to grasslands influences fire frequency and sensitivity to climate variability in ponderosa pine forests of the Colorado Front Range. International Journal of Wildland Fire 21:562–571.

Hansen, M. C., P. V Potapov, R. Moore, M. Hancher, S. a Turubanova, A. Tyukavina, D. Thau, S. V Stehman, S. J. Goetz, T. R. Loveland, A. Kommareddy, A. Egorov, L. Chini, C. O. Justice, and J. R. G. Townshend. 2013. High-resolution global maps of 21st-century forest cover change. Science 342:850–853.

Hayward, G. D., T. T. Veblen, L. H. Suring, and B. Davis. 2012. Challenges in the application of historical range of variation to conservation and land management. Pages 32–45 *in* J. A. Wiens, G. D. Hayward, H. D. Safford, and C. Giffen, editors. Historical Environmental Variation in Conservation and Natural Resource Management. Wiley-Blackwell, Hoboken, NJ.

Homer, C. G., J. A. Dewitz, L. Yang, S. Jin, P. Danielson, G. Xian, J. Coulston, N. D. Herold, J. D. Wickham, and K. Megown. 2015. Completion of the 2011 National Land Cover Database for the conterminous United States-Representing a decade of land cover change information. Photogrammetric Engineering and Remote Sensing 81:345–354.

Horning, N. 2010. Random Forests: An algorithm for image classification and generation of continuous fields data sets. Pages 1–6 International Conference on Geoinformatics for Spatial Infrastructure Development in Earth and Allied Sciences. Hanoi, Vietnam.

Hothorn, T., K. Hornik, and A. Zeileis. 2014. party : A Laboratory for Recursive Part(y)tioning.

Kaufmann, M. R., T. Veblen, and W. H. Romme. 2006. Historical Fire Regimes in Ponderosa Pine Forests of the Colorado Front Range, and Recommendations for Ecological Restoration and Fuels Management. Front Range Fuels Treatment Partnership Round Table, Findings of the Ecology Workgroup. Fort Collins, CO.

Kitzberger, T., P. M. Brown, E. K. Heyerdahl, T. W. Swetnam, and T. T. Veblen. 2007. Contingent Pacific-Atlantic Ocean influence on multicentury wildfire synchrony over western North America. Proceedings of the National Academy of Sciences of the United States of America 104:543–548.

Kuhn, M. 2015. A Short Introduction to the caret Package:1–10.

Mast, J. N., T. T. Veblen, and M. E. Hodgson. 1997. Tree invasion within a pine/grassland ecotone: An approach with historic aerial photography and GIS modeling. Forest Ecology and Management 93:181–194.

Matthews, L. E. 2005. Historical Imagery Holdings For The United States Department of Agriculture. https://www.fsa.usda.gov/Internet/FSA_File/vault_holdings2.pdf.

Millar, C. I., N. L. Stephenson, and S. L. Stephens. 2007. Climate Change and Forests of the Future: Managing in the Face of Uncertainty. Ecological Applications 17:2145–2151.
National Elevation Dataset, United States Geological Survey. 1999. . nationalmap.gov/elevation.html.
Platt, R. V., and T. Schoennagel. 2009. An object-oriented approach to assessing changes in tree cover in the Colorado Front Range 1938-1999. Forest Ecology and Management 258:1342–1349.
Raffa, K. F., B. H. Aukema, B. J. Bentz, A. L. Carroll, J. a. Hicke, M. G. Turner, and W. H. Romme. 2008. Cross-scale Drivers of Natural Disturbances Prone to Anthropogenic Amplification: The Dynamics of Bark Beetle Eruptions. BioScience 58:501.
Rhemtulla, J. M., R. J. Hall, E. S. Higgs, and S. E. Macdonald. 2002. Eighty Years of Change: Vegetation in the Montane Ecoregion of Jasper National Park, Alberta, Canada. Canadian Journal of Forest Research 32:2010–2021.
Rocca, M. E., P. M. Brown, L. H. MacDonald, and C. M. Carrico. 2014. Climate change impacts on fire regimes and key ecosystem services in Rocky Mountain forests. Forest Ecology and Management 327:290–305.
Rollins, M. G. 2009. LANDFIRE: A nationally consistent vegetation, wildland fire, and fuel assessment. International Journal of Wildland Fire 18:235–249.
Schoennagel, T., R. L. Sherriff, and T. T. Veblen. 2011. Fire history and tree recruitment in the Colorado Front Range upper montane zone: Implications for forest restoration. Ecological Applications 21:2210–2222.
Sherriff, R. L., R. V Platt, T. T. Veblen, T. L. Schoennagel, and M. H. Gartner. 2014. Historical, Observed, and Modeled Wildfire Severity in Montane Forests of the Colorado Front Range. PloS one 9:1–17.
Sherriff, R. L., and T. T. Veblen. 2006. Ecological Effects of Changes in Fire Regimes in Pinus ponderosa Ecosystems in the Colorado Front Range. Journal of Vegetation Science 17:705–718.
Sherriff, R. L., and T. T. Veblen. 2007. A spatially-explicit reconstruction of historical fire occurrence in the ponderosa pine zone of the Colorado front range. Ecosystems 10:311–323.
Sherriff, R. L., and T. T. Veblen. 2008. Variability in Fire-Climate Relationships in Ponderosa Pine Forests in the Colorado Front Range. International Journal of Wildland Fire 17:50–59.
Sibold, J. S., T. T. Veblen, and M. E. González. 2006. Spatial and temporal variation in historic fire regimes in subalpine forests across the Colorado Front Range in Rocky Mountain National Park, Colorado, USA. Journal of Biogeography 33:631–647.
Swetnam, T. W., C. D. Allen, and J. L. Betancourt. 1999. Applied historical ecology: using the past to manage for the future. Ecological applications 9:1189–1206.
Turner, M. G. 2010. Disturbance and Landscape Dynamics in a Changing World. Ecology 91:2833–2849.
Veblen, T. T., and J. A. Donnegan. 2005. Historical range of variability for forest vegetation of the national forests of the Colorado Front Range. USDA Forest Service. Golden, CO.
Veblen, T. T., T. Kitzberger, and J. Donnegan. 2000. Climatic and human influences on fire regimes in ponderosa pine forests in the colorado front range. Ecological Applications 10:1178–1195.
Veblen, T. T., and D. C. Lorenz. 1986. Anthropogenic Disturbance and Recovery Patterns in Montane Forests, Colorado Front Range. Physical Geography 7:1–24.
Veblen, T. T., and D. C. Lorenz. 1991. The Colorado Front Range: A century of ecological change. University of Utah Press, Salt Lake City, UT.
Williams, M. A., and W. L. Baker. 2012. Spatially extensive reconstructions show variable-severity fire and heterogeneous structure in historical western United States dry forests. Global Ecology and Biogeography 21:1042–1052.

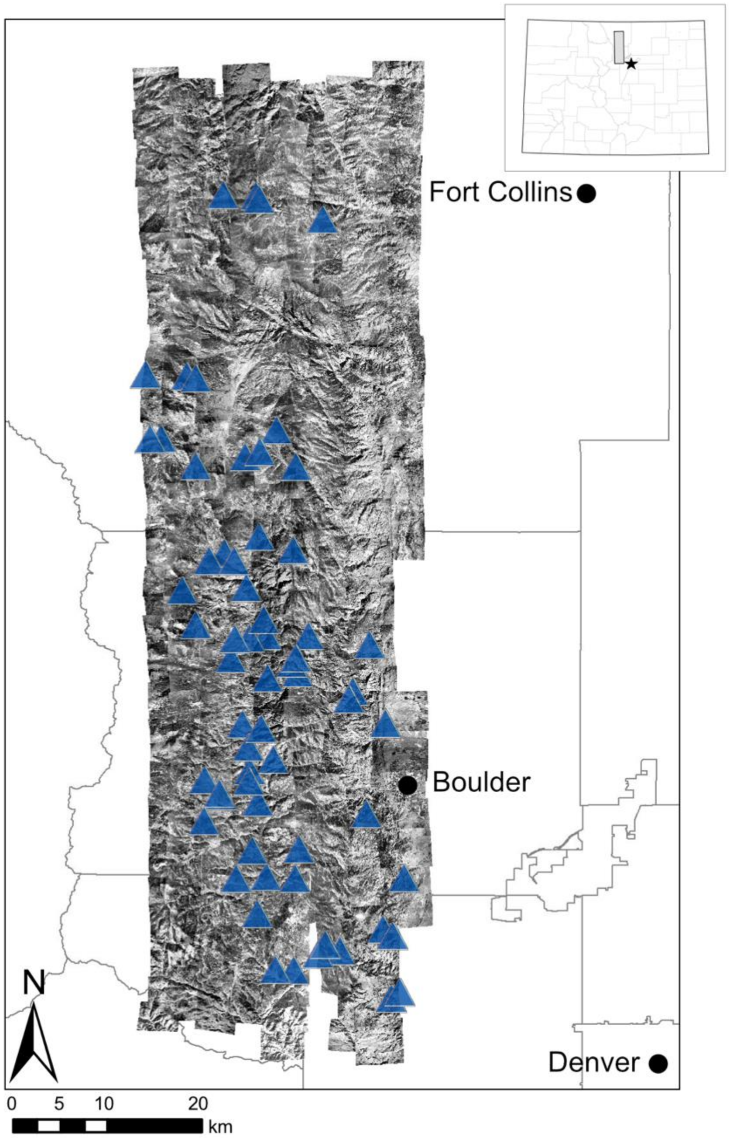

Figure 1: Map showing the extent of selected historical (1938, 1940) air photos in the northern Front Range, CO. Sites of paired fire scar records and stand age data included in the Sherriff et al. (2014) analysis and overlapping with the study area (n = 66) are shown in blue, and county perimeters are outlined in grey.

Table 1: Description of historical air photo locations and time periods of collection for each of the counties included in the study area.

County	Number of Images	Time Period
Boulder	114	May 1938, Oct 1938, Oct 1940
Clear Creek	1	Oct 1938
Gilpin	30	Oct 1938
Jefferson	14	May 1938, Oct 1938, Oct 1940
Larimer	149	May 1938, Oct 1938, Oct 1940
All	308	

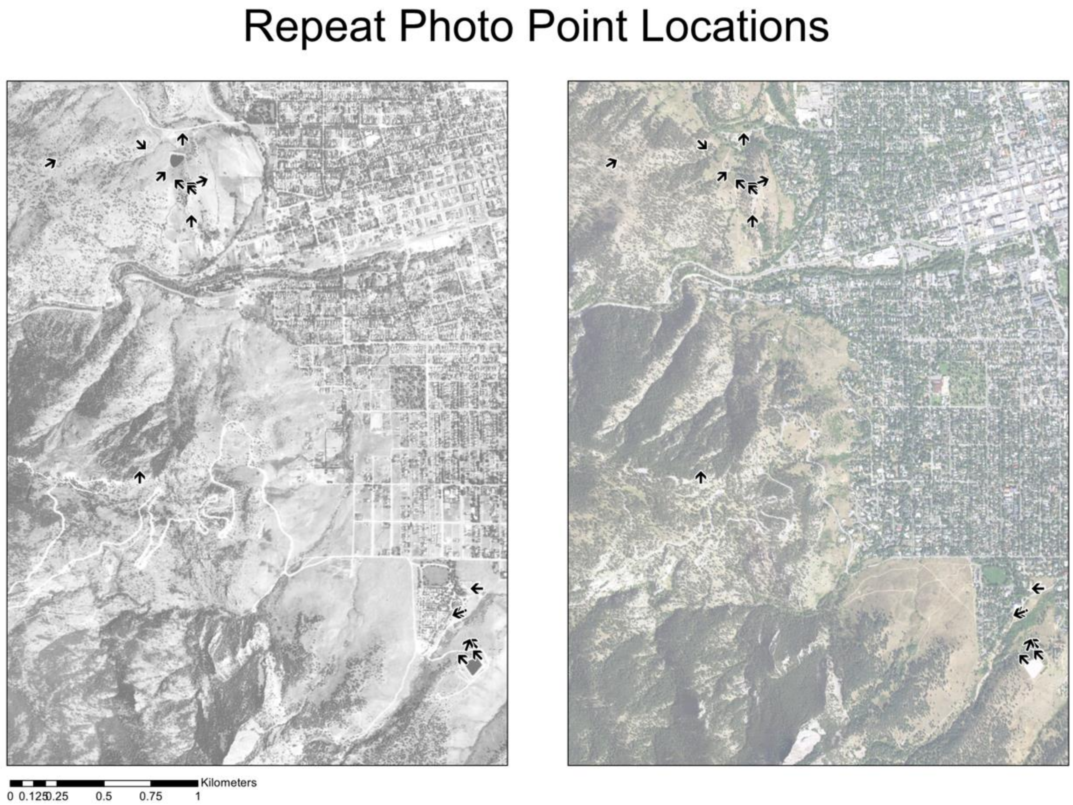

Figure 2: Location and direction of repeat photo points overlain on 1938 (left) and 2015 (right) aerial imagery

Table 2: Overview of repeat photos collected on OSMP properties near Boulder, CO. “Slide Number” corresponds to page number in Appendix A.

Slide Number	Photo Code	Location	Scene/Name of Location	Original Photographer	Year of Historical Image	Easting (m)	Northing (m)	Azimuth (deg)	Elevation (m)
2	MCC-306	Chautauqua	Chautauqua Auditorium, VW of Mt Sanitas	McClure	1900-1910	476204	4427284	315	1788
3	MCC-306	Chautauqua	Chautauqua Auditorium, VW of Mt Sanitas	McClure	1900-1910	476179	4427345	315	1773
4	MCC-306	Chautauqua	Chautauqua Auditorium, VW of Mt Sanitas	McClure	1900-1910	476179	4427345	315	1773
5	X-11711	Chautauqua	Chautauqua Auditorium, VW of Mt Sanitas	Unknown	1900-1910	476125	4427260	315	1789
6	X-11711	Chautauqua	Chautauqua Auditorium, VW of Mt Sanitas (2) Cropped	Unknown	1900-1910	476125	4427260	315	1789
7	X-11711	Chautauqua	Chautauqua Auditorium, VW of Mt Sanitas (2) Cropped	Unknown	1900-1910	476125	4427260	315	1789
8	X-11711	Chautauqua	Chautauqua Auditorium, VW of Mt Sanitas (2) Cropped	Unknown	1900-1910	476125	4427260	315	1789
9	MCC-4852	Chautauqua	Boulder from Chautauqua right side panoramic	McClure	1900-1910	476152	4427337	20	1771
10	MCC-4852	Chautauqua	Boulder from Chautauqua right side panoramic	McClure	1900-1910	476152	4427337	20	1771
11	X-11723	Chautauqua	Chautauqua Tents, VW of Flat Irons	Robert Collier	c. 1897	476114	4427511	250	1754
12	X-11723	Chautauqua	Same Chautauqua Tents, VW of Flat Irons	Robert Collier	c. 1897	476101	4427505	250	1754
13	MCC-305	Chautauqua	Chautauqua Auditorium, VW of Flat Irons	McClure	c. 1905	476203	4427642	270	1738
14	MCC-305	Chautauqua	Same Chautauqua Auditorium, VW of Flat Irons	McClure	c. 1905	476199	4427637	270	1743
15	208-2-16photo_6	Red Rocks	Vw East of Mapleton School	JB Sturtevant	c 1898	474734	4429805	70	1749
16	208-4-23Photo_2	Red Rocks	Constructing Bo City Reservoir, So. Of Mt Sanitas	JB Sturtevant	1875	484640	4434976	10	1750
17	208-4-23Photo_5	Red Rocks	Duplicate Constructing Bo City Reservoir, So. Of Mt Sanitas	JB Sturtevant	1875	484640	4434976	10	1750
18	208-4-23Photo_7	Red Rocks	Bo City Reservoir, SW of Sanitarium, recently constructed	JB Sturtevant	1876-1899	484640	4434976	10	1750
19	208-4-23Photo_8	Red Rocks	Bo City Reservoir water beginning to flow	JB Sturtevant	1876-1899	484640	4434976	10	1750
20	208-4-23photo_12	Red Rocks	BoCity Reservoir with chain link fence	JB Sturtevant	1876-1899	474517	4429831	45	1739
21	208-4-23photo_15	Red Rocks	BoCityRes & Sunshine	JB Sturtevant	1875-1899	474679	4429774	315	1742
22	s-939	Red Rocks	BoCityRes& lower Sunshine, women in foreground	JB Sturtevant	1875-1899	474614	4429789	315	1735
23	208-4-23photo_16	Red Rocks	BoCityRes & Sunshine	JB Sturtevant	1875-1899	474679	4429774	315	1742
24	208-4-23photo_3; S-941	Red Rocks	BoCity Res&RedRocks	JB Sturtevant	1876-1899	474412	4429998	135	1751
25	208-4-23photo_3; S-941	Red Rocks	BoCity Res&RedRocks	JB Sturtevant	1876-1899	474412	4429998	135	1751
26	208-4-22_photo_1	Red Rocks	RedRocks View of Sunshine Canyon	JB Sturtevant	1897-2016	474681	4429759	315	1761
27	K-250	Red Rocks	Red Rocks, south side	Donald C Kemp	1943	474679	4429592	0	1719
28	BHS 208-P-3	Red Rocks	Red Rocks from Brierly Mountain	WH Jackson	1893-2016	473929	4429901	60	1930
29	BHS 208-P-3	Red Rocks	Red Rocks from Brierly Mountain	WH Jackson	1893-2016	473929	4429901	60	1930
30	BHS 208-P-3	Red Rocks	Red Rocks from Brierly Mountain	WH Jackson	1893-2016	473929	4429901	60	1930
31	BPL C 208-4-22photo_4	Red Rocks	Red Rocks view of South end of Mt. Sanitas	JB Sturtevant	1897-2016	474632	4430027	0	1693
32	X-11665	Flagstaff Mountain	From Flagstaff Mtn --view of red rocks	AE Dickerson	1905-1910	474404	4428229	0	2036
33	X-11665	Flagstaff Mountain	From Flagstaff Mtn --view of red rocks	AE Dickerson	1905-1910	474404	4428229	0	2036

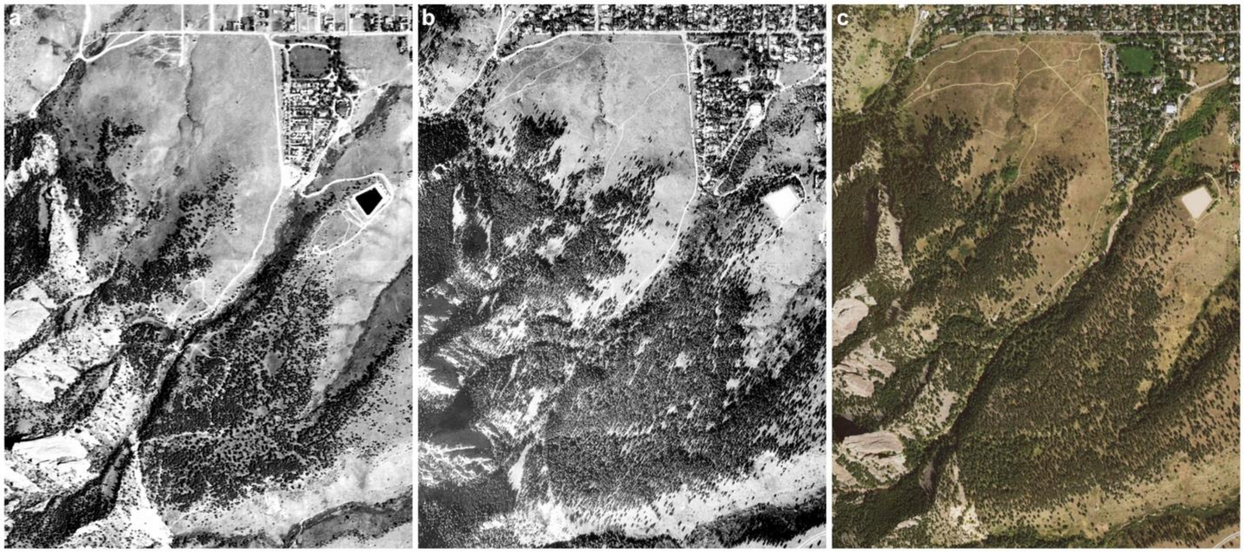

Figure 3: A comparison of 1938 (a), 1999 (b), and 2015 (c) aerial imagery covering Chautauqua and the first, second, and third flatirons.

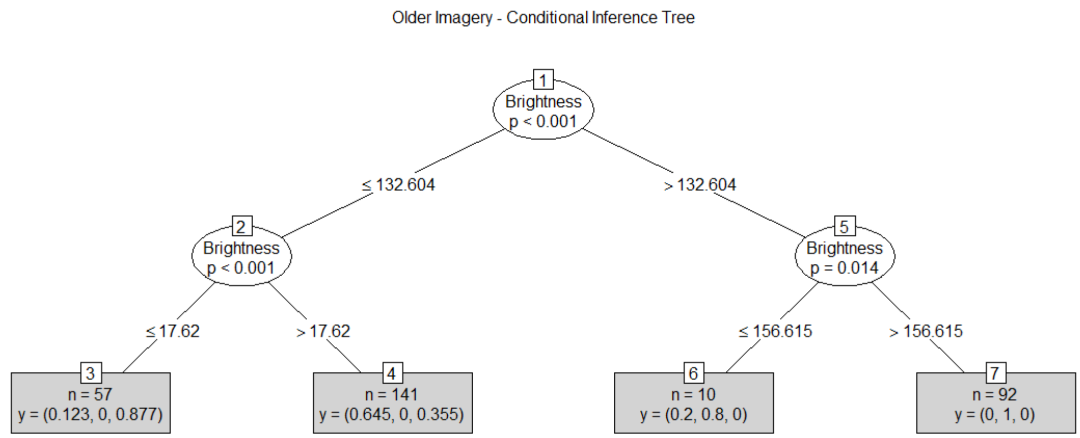

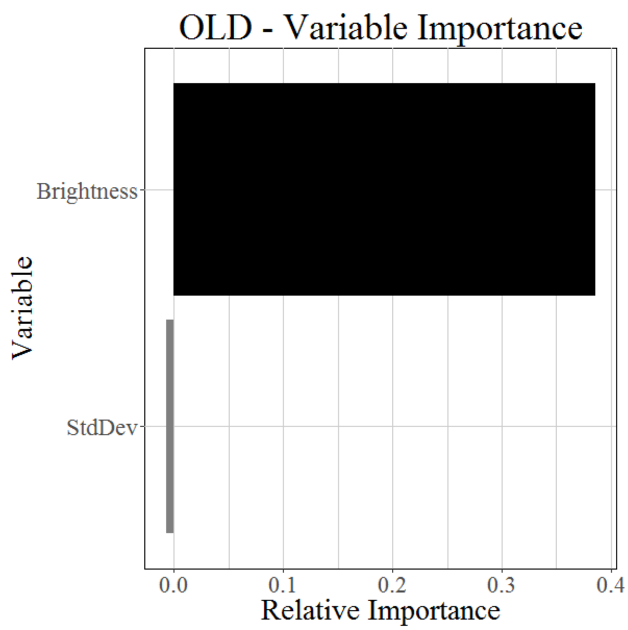

OLD	Forest	Non-Forest	Water/ Shadow	SUM	User's Accuracy
Forest	80	18	2	100	0.80
Non-Forest	1	99	0	100	0.99
Water/ Shadow	58	0	42	100	0.42
SUM	139	117	44	300	
Producer's Accuracy	0.58	0.85	0.95		0.74

Confusion matrix for preliminary pixel-based classification of historical imagery. Final classification used the thresholds defined above, and the minimum observed variance in training pixels of the forest class to separate the three cover types.

Figure 4: Diagram of decision tree classification, results of the conditional inference framework, and classification accuracy assessment based on decision-tree classification for high-resolution historical air photos collected by the US Forest Service ca. 1938. Nodes with two paths below them represent a binary split in the data based on the specified variable and values. N is the number of training pixels placed in a terminal node. The “y” vector in each terminal node represents the proportion of pixels from each class in this bin, where the first value is forest, the second is bare ground, and the third is water/shadow. Variable importance refers to mean decrease in classification accuracy when removing a variable from the conditional inference model.

Change in Forest Cover on OSMP Properties (1938-2015)

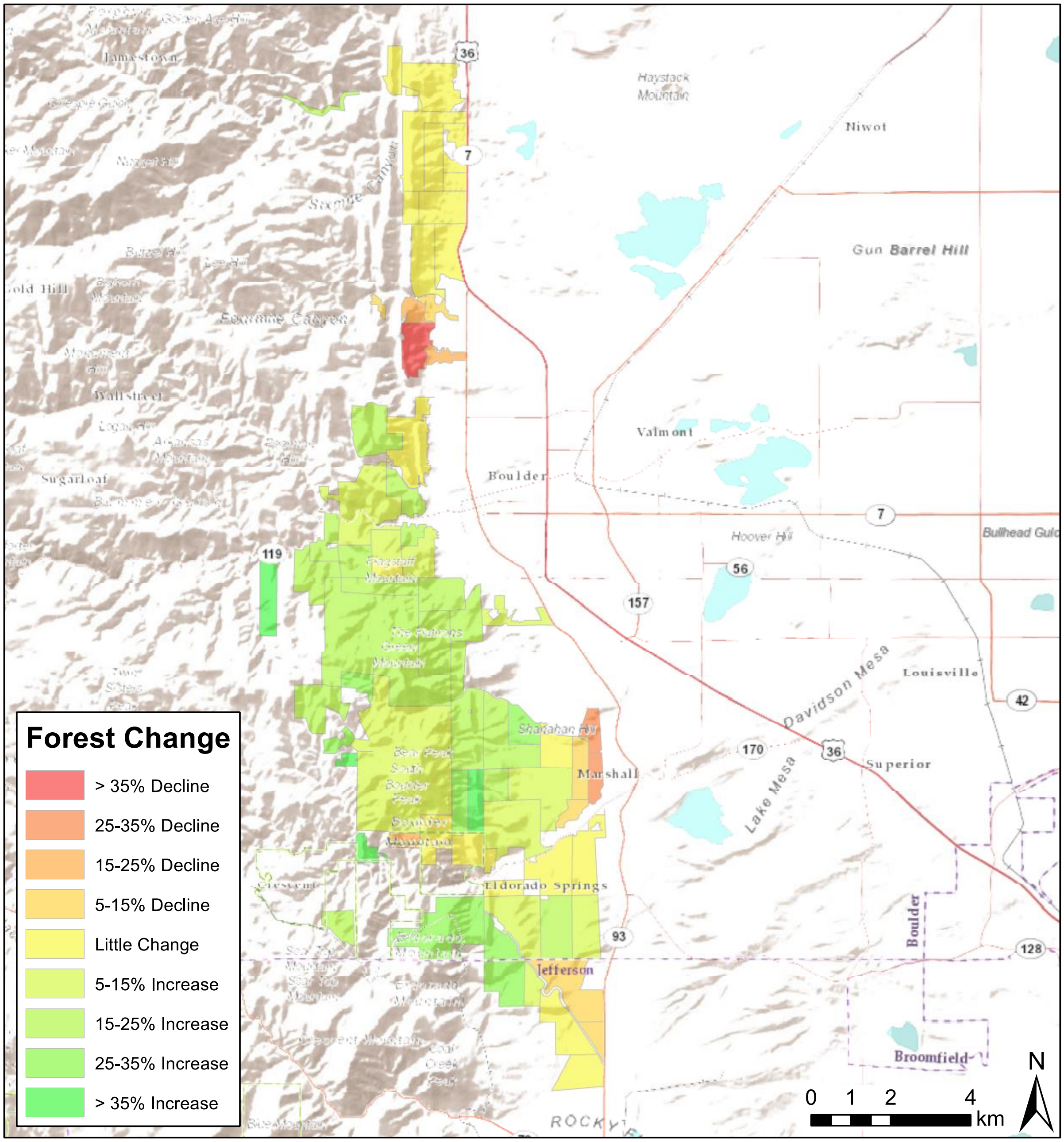

Figure 5: Map of forest change on selected OSMP properties surrounding Boulder, CO. Properties were included in the analysis if: (i) they included visible forest cover in at least one time period, and (ii) if 1938 imagery was available for a given parcel. Percent change is calculated as proportion of forest cover in the parcel in 2015 minus the proportion of forest cover in 1938.

Table 3: Overview of selected OSMP properties and results of pixel-based forest classification for each time period -1938 and 2015.

Property Name	Percent Forest 1938	Percent Forest 2015	Forest Change
AMERICAN PARK	64.54	78.54	14.00
ANDERSON-DEBACKER	29.28	58.82	29.54
AUSTIN - RUSSELL	30.60	47.04	16.44
BAIRD	42.52	63.29	20.77
BARUT (THE MATRON)	59.93	56.18	-3.75
BEECH - West	10.45	11.25	0.79
BEECH, COUNTY	5.18	4.52	-0.66
Benedictine Abbey	16.98	42.24	25.26
BERGHEIM - WOOD	40.36	57.67	17.31
BOULDER GREENS VENTURE	11.37	9.78	-1.59
BOULDER MEMORIAL HOSPITAL	16.89	17.18	0.29
BUCKINGHAM PARK	25.35	33.49	8.14
BUFFALO PARK CE	52.22	76.32	24.10
BUSSE	22.06	57.89	35.83
CAMPBELL	65.81	63.54	-2.28
CULBERSON	28.69	68.32	39.62
DOVER-BLACKER	9.93	0.38	-9.55
DUNN I	7.75	20.04	12.28
DUNN II	8.62	6.07	-2.55
ELDORADO MOUNTAIN (CONDA QUARRY)	43.37	68.63	25.26
ENCHANTED MESA	38.18	55.48	17.31
ERNI	43.30	8.92	-34.38
FLATIRONS VISTA	3.56	15.08	11.52
FOOTHILLS BUSINESS PARK	1.94	0.19	-1.75
FOOTHILLS BUSINESS PARK CE	2.24	1.50	-0.73
FRASIER FARMS	21.27	43.40	22.13
HEDGECOCK	32.30	19.32	-12.98
HOGAN RANCH - (CE)	15.33	11.99	-3.35
HOLMES	18.21	33.70	15.49
JEWEL MOUNTAIN LAND CO.	3.30	2.28	-1.02
JODER II	9.27	6.11	-3.16
KASSLER	27.15	51.04	23.89
KINEMAN	29.28	55.47	26.18
LAINGOR	41.37	75.16	33.79

LINDSAY - West	32.79	46.21	13.42
LINDSAY / JEFFCO	21.74	51.39	29.65
MANN - West	4.41	0.26	-4.15
MASSEY / QUARTER CIRCLE V	79.71	55.22	-24.48
McCANN, G - North	22.63	27.15	4.52
MOORE FAMILY	26.83	26.53	-0.30
MOORE, MARY I	12.44	1.60	-10.84
N. I. S. T. CE	10.58	17.18	6.60
NCAR PARK	26.60	41.64	15.04
NEJEZCHLEB	17.39	19.30	1.90
PARSONS	6.73	2.41	-4.31
RICE BE	20.55	56.22	35.66
RUDD - West	6.13	4.86	-1.26
SCHNEIDER	4.98	1.64	-3.34
SCHNELL I	50.39	73.25	22.86
SCHNELL II	51.97	68.41	16.44
SHANAHAN, SOUTH CE	30.19	2.70	-27.50
SIGNORELLA CE	64.90	55.34	-9.56
STATE PATENT - PANORAMA	30.00	42.98	12.98
STENGEL I	4.44	10.69	6.25
STENGEL II	18.66	35.76	17.09
STOY	33.60	51.84	18.24
THOMAS, HOGAN, PARRISH (T.H.P.) - West	40.66	12.24	-28.42
TRAM HILL	39.52	71.52	32.01
US PATENT - BEAR PEAK	56.19	61.29	5.10
US PATENT - GREEN MTN.	50.29	64.86	14.57
VAN VLEET / JEFFERSON COUNTY	7.19	5.29	-1.90
WELLS - East	30.10	47.28	17.18
WELLS - West	48.34	65.23	16.90
WITTEMYER I - North	40.49	63.08	22.58
WONDERLAND HILL DEV CORP I	29.81	8.43	-21.38
Total	**31.07**	**40.33**	**9.25**

Figure 6: Some of the issues with merging adjacent air photos into a single photo mosaic. (a) Visible tonal differences at scene edges following mosaicking in the eastern flight line, and uncorrected offset between adjacent flight lines (b). Frame (b) will ultimately look like (a), and the full mosaic will then be tonally corrected in Adobe Photoshop CS6. However, image segmentation also corrects for some of these tonal differences in the classification process.

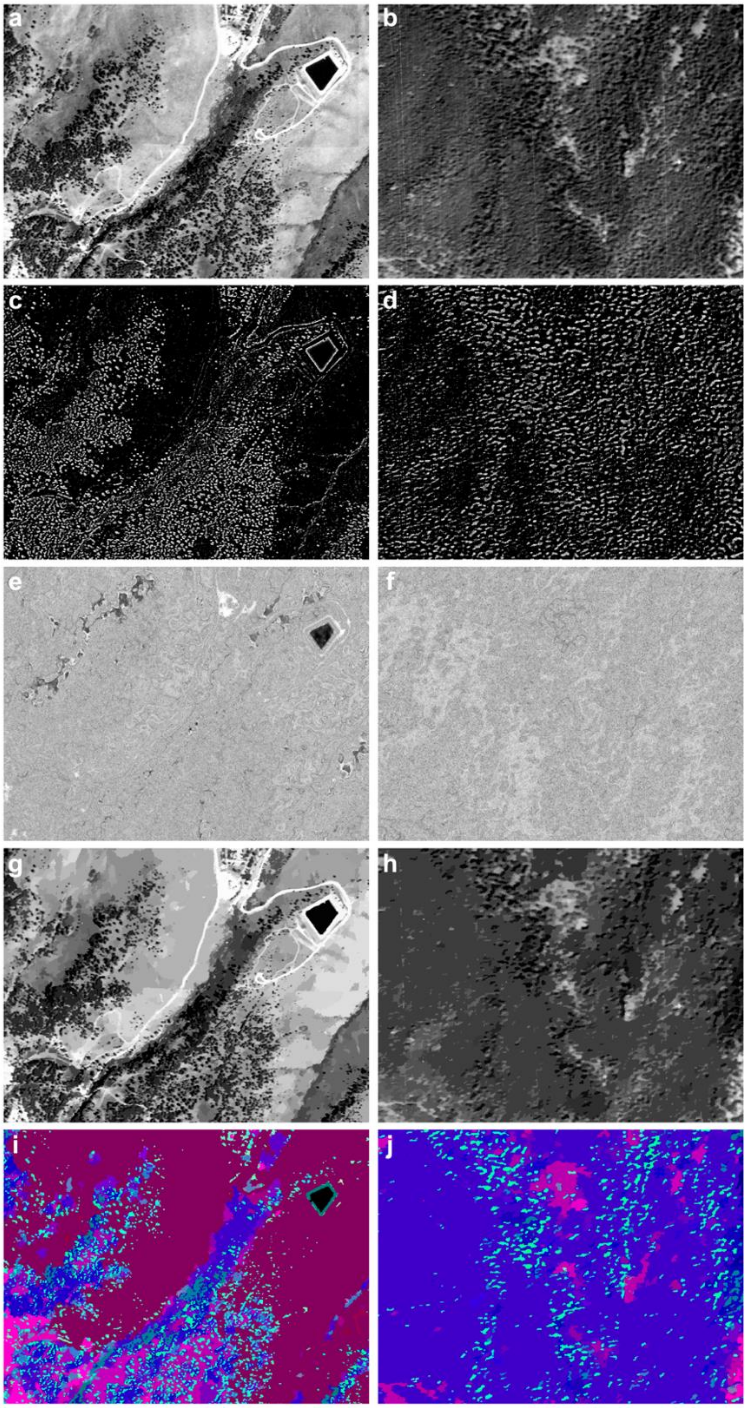

Figure 7: An overview of proposed image classification techniques in areas of sparse (left) and dense (right) forest cover. Original imagery (a, b) is processed using an expanding window method to identify dark pixels surrounded by lighter ones (c, d), and describe the variance around each pixel (e, f). Images are then segmented to identify areas of relatively similar appearance. This segmentation can be completed solely based on image brightness (g, h), or based on image brightness, locally dark areas, and variance combined (i, j). These segmented areas can then be classified using machine learning techniques such as random forests or support vector machines.